Progress In Electromagnetics Research C, Vol. 97, 95–107, 2019

Double-Elliptical Shaped Miniaturized Microstrip Patch Antenna for Ultra-Wide Band Applications

Jerry V. Jose[1, *], Aruldas S. Rekh[1], and Manayanickal J. Jose[2]

Abstract—Greater design flexibility and newer miniaturization techniques are highly sought after by the commercial antenna industry and researchers. Micro-Strip Patch Antenna (MSPA) is finding huge applications in various fields of communication. In the present paper, the novel idea of Double-Elliptical Micro-strip Patch Antenna (DEMPA) is proposed for antenna miniaturization and higher design flexibility. Double-Elliptical Patch (DEP) is made as the combination of two half-elliptical patches having the same minor axis and different semi-major axes or the same major axis and different semi-minor axes. A DEP with different lengths of horizontally arranged semi-major axes and centrally given feed was considered here. The length of semi-major axis for right half-elliptical patch was varied while keeping the length of semi-major axis for left half-elliptical patch fixed. Design of DEMPA was carried out using Ansoft HFSS software, and the antenna has been fabricated and tested. The measured results were in good agreement with the simulated ones. The percentage reduction in effective patch area was found to be 8.33 for DEMPA compared to the corresponding elliptical patch antenna. The DEMPA covered the entire frequency range of Ultra Wide Band (UWB). With this novel shape, greater design flexibility along with miniaturization is achieved. The axial ratio analysis showed that the resulted antenna was of linear polarization.

1. INTRODUCTION

Micro-Strip Patch Antenna (MSPA) finds immense applications in the fields of Global Positioning System (GPS), mobile and satellite communications, Radio Frequency Identification (RFID), radar communications, telemedicine, radiolocation services, holographic antennas, Wireless Local Area Network (WLAN), and many more. Apart from being inexpensive, easy to manufacture, light in weight, of thinner profile, and capable of producing linear and circular polarizations, the MSPAs can be made of practically any shape. The performance parameters of MSPAs may be largely varied by adopting different shapes for them. Most popular shapes for MSPAs are the basic regular geometric shapes such as rectangle, circle, triangle, and ellipse and their variants. Patches are also made of fractals which are never ending and self-similar patterns that repeat themselves at different scales.

Out of the regular geometric shapes, Elliptical Micro-strip Patch Antenna (EMPA) is the least explored one because of the complexity involved in its design due to the presence of Mathieu and Bessel functions. EMPAs are able to generate circular polarizations with only a single feed arranged along a radial line inclined at $\pm 45^\circ$ to its major axis [1] while the rectangular MSPAs need multiple feeds or substantial shape variations to develop circular polarization. Another important advantage of EMPA is the dual resonant frequencies of the dominant even and odd modes [2]. The design flexibility of EMPA is better because of a higher degree of freedom due to eccentricity which is defined as the ratio of semi-minor axis to semi-major axis of ellipse. For a circle, the eccentricity is one and it varies between

Received 20 September 2019, Accepted 19 November 2019, Scheduled 29 November 2019
* Corresponding author: Jerry V. Jose (jerryv@karunya.edu.in).
[1] Karunya Institute of Technology and Sciences, Coimbatore, Tamil Nadu, India. [2] Govt. College of Engineering Kannur, Kerala, India.

zero and one for an ellipse. When the patch becomes only slightly elliptical (eccentricity being less than 10%–20% with respect to unity), best circular polarization is attained [3].

Several variants of elliptical shape were proposed for the MSPA. Elliptical patch with slots of circular arcs at different locations was used along with frequency selective surface superstrate [4]. Performance of patches with two and four such slots respectively was studied. Elliptical patch slotted with single circular arc was tried by another researcher also [5]. The use of carved semi-elliptical parasitic patch helped to achieve wider bandwidth [6]. Here, the main patch, parasitic patch and truncated ground plane were in the shape of half-ellipse. The literature indicates that hybrid trapezoidal-elliptical patch where the lower portion of elliptical patch was overlapped by a trapezoidal patch could enhance the impedance bandwidth [7]. Fractal elliptical monopole antenna which resembled the Lorenz fractal shape was proposed [8]. Elliptical shaped fractal patch antenna for multi-band applications was also designed [9]. Two such ellipses were joined at an angle of 45° to design the patch. Three orthogonal sector slots were included on elliptical patch to obtain less effective patch area and higher bandwidth [10]. Within an elliptical patch, two slots were incorporated at its edges and as a modification these two slots were combined into one slot [11]. Two L-shaped slots were made in elliptical patch to design antenna for UWB applications [12]. Egg shaped and heart shaped patches were developed from the basic elliptical patch for WiMAX applications [13]. Semi-elliptical patch was made out of rectangular patch by truncating its sides for UWB applications [14]. A circular disc was removed from the elliptical patch and the resulting shape was like a crescent [15]. The effective patch area was reduced by 40% and similar radiation properties as that of full elliptical patch were retained. The shape of antenna with an elliptical patch inserted within an elliptical slot was also proposed [16]. A slot was introduced along the major axis of an elliptical patch [17]. Semi-elliptical patch with a semi-circular ring slot was suggested for MSPA [18]. Patch antenna was made in the shape of confocal elliptical annular ring [19]. Elliptical annular ring patch antenna was also developed [20]. Amorphous shaped patches were generated for MSPA from ellipse [21]. Elliptical patch with its edges truncated parallel to its major axis could reduce the effective patch area and improve impedance bandwidth [22]. When two symmetrical slots were loaded on to elliptical patch, impedance bandwidth and gain were improved and the effective patch area was reduced substantially [23]. When the axial ratio falls within the range of 0–3 dB, the polarization is practically considered to be circular and beyond that it is linear. EMPA can produce linear polarization also, and performance study of linearly polarized elliptical patch antenna is a less explored area even though much research work was done for linearly polarized rectangular and circular patches [24].

There are a lot of high quality research works going on the development of electromagnetic devices, other than that related to MSP antennas. Some of the researchers are recently concentrating on the use of antenna in the fields of Industrial, Scientific and Medical (ISM) [25], planar array for Wi-fi applications [26, 27] and cancer diagnosis [28]. Use of metamaterials for better performance of low profile antennas [29] and improving image quality [30] are explored by many. The electromagnetic properties of nano-metal-coated textile surfaces are investigated recently [31]. Work on designing the Electromagnetic Band Gap (EBG) structures for microwave imaging applications [32] is also reported. Analysis of polarization conversion properties of chiral metamaterials [33], and electromagnetic wave absorption properties of construction materials [34] are some among the promising research fronts in electromagnetics.

Coming back to MSPAs, it is commercially very much significant to find ways or techniques to reduce the effective patch area of MSPA while retaining its radiation properties. For EMPA, the volume of work reported in literature towards antenna miniaturization is less.

The more the degrees of freedom are, the higher the flexibility will be in antenna design. Antenna miniaturization is a highly sought after commercial aspect. The basic regular geometrical shape of ellipse may be investigated for the possibilities of having more degrees of freedom and further miniaturization. Such an exploration helped us to propose a modified form of ellipse, called 'double-ellipse'. The Double-Elliptical Patch (DEP) is made as the combination of two half-elliptical patches having the same minor axis and different semi-major axes or the same major axis and different semi-minor axes. In the present paper, the novel idea of Double-Elliptical Micro-strip Patch Antenna (DEMPA) is proposed for antenna miniaturization. A DEP with different lengths of horizontally arranged semi-major axes and centrally given feed was considered here. The length of semi-major axis for right hand side of DEP was varied while keeping the length of semi-major axis for left hand side fixed. Design of DEMPA was carried

out using Ansoft HFSS and the antenna has been fabricated and tested. The measured results were in good agreement with the simulated results. With this novel shape, greater design flexibility along with miniaturization is achieved. The axial ratio analysis showed that the resulted antenna was of linear polarization.

2. CONSTRUCTION DETAILS OF DOUBLE-ELLIPTICAL PATCH

As stated above, double-ellipse is a combination of two half-ellipses of having the same minor axis and different semi-major axes or the same major axis and different semi-minor axes. A regular elliptical patch has two axes of symmetry, but a DEP has only one. If the minor axis is the same for two half-elliptical patches, then direction of major axes becomes the axis of symmetry. If direction of minor axes is the axis of symmetry, then the two half-elliptical patches would have the same major axis. Orientation of the axis of symmetry, i.e., horizontal, vertical or inclined at certain angle to horizontal, is also significant as it would affect the radiation properties. Hence, in the context of antenna design, a DEP may be classified according to the axis of symmetry and its orientation. In other words, we need to specify the axis of symmetry and its orientation to define a DEP. Let the DEP with axis of symmetry along the direction of major axes be denoted as DEP_{ma} and the DEP with axis of symmetry along the direction of minor axes be denoted as DEP_{mi}. The construction details of DEP are shown in Fig. 1.

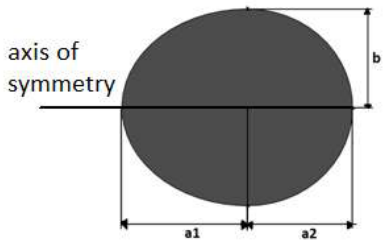

Figure 1. Construction details of double-elliptical patch.

Effective patch area (A_p) of DEP_{ma} can be expressed as,

$$A_{pma} = \frac{\pi}{2} b\,(a_1 + a_2) \tag{1}$$

where b = length of the common semi-minor axis of the two half-elliptical patches, a_1 = length of the semi-major axis of first half-elliptical patch, and a_2 = length of the semi-major axis of second half-elliptical patch. Effective patch area for DEP_{mi} is,

$$A_{pmi} = \frac{\pi}{2} a\,(b_1 + b_2) \tag{2}$$

where a = length of the common semi-major axis of the two half-elliptical patches, b_1 = length of the semi-minor axis of first half-elliptical patch, and b_2 = length of the semi-minor axis of second half-elliptical patch. The design of DEMPA possesses one additional degree of freedom compared to that of EMPA.

3. ANTENNA DESIGN AND FABRICATION

3.1. Antenna Geometry

For the present work, an EMPA for UWB communications with lengths of semi-major axis and semi-minor axis as 9.0 mm and 7.0 mm respectively was chosen as a reference [17]. Its major axis was arranged horizontally. In the present study, the axis of symmetry of DEP was directed along the horizontal major axes and hence it may be denoted as DEP_{ma}. It consisted of an LHS half-elliptical patch (first patch) and an RHS half-elliptical patch (second patch) with the common vertical minor axis of length 14 mm. The a_1 was fixed at 9 mm and a_2 was varied as 8.5 mm, 8.0 mm, and 7.5 mm. For a_2 = 7.0 mm, the

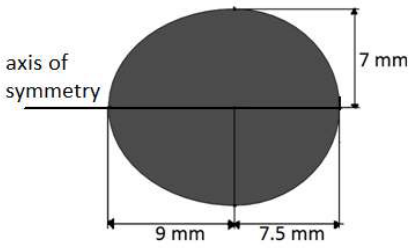

Figure 2. The geometry of DEP_{ma}.

right half-ellipse becomes a half-circle of radius 7.0 mm and for $a_2 < 7.0$ mm, the minor axis of the right half-ellipse becomes its major axis. This will increase the level of asymmetry between the right and left half-ellipses and hence the scope of this present study has been restricted to the range (7.0 mm $< a_2 <$ 9.0 mm). Also, there is no point in taking values of $a_2 > 9.0$ mm as it will not contribute to miniaturization. The DEMPA with a_2 of 7.5 mm was fabricated and tested. The geometry of DEP is shown in Fig. 2.

3.2. Design Using HFSS

The High Frequency Structure Simulator (HFSS), a modeling and simulation software from Ansoft, was used to develop model for the DEMPA. The material of substrate used was FR-4, with a relative dielectric constant, $\varepsilon_r = 4.4$ and thickness, $h = 1$ mm. The length (L) and width (W) of substrate were 40 mm and 38 mm respectively. The micro-strip feed line has width of 1.6 mm and length of feed was 20.7 mm. The dimensions of ground plane were 38 mm and 20 mm. The DEP and ground plane were modeled with the same metallic material. Using HFSS, full wave electromagnetic simulations were carried out to analyze the different performance parameters such as Return Loss, VSWR and Gain. Radiation patterns and surface current distributions were also obtained from simulations at the resonant frequencies.

3.3. Fabrication and Testing

The DEMPA with $a_2 = 7.5$ mm was fabricated and tested. For feeding the prototype antenna, an SMA connector with characteristic impedance of 50 Ω was used. The SMA connector was joined to the substrate through the process of welding. A micro-strip feed line of width 1.6 mm and length 20.7 mm was placed at the centre of the patch. Return Loss and VSWR measurements were taken at a lossless laboratory. The Vector Network Analyzer ENA (E 5071C) was used to obtain the return loss and VSWR characteristics. The simulated and measured results were in good agreement within the range from 3.07 GHz to 17.669 GHz. The top view and bottom view of the fabricated DEMPA are shown in Fig. 3.

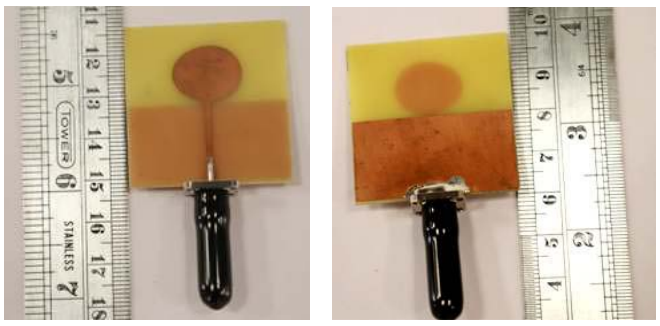

(a) (b)

Figure 3. Fabricated DEMPA (a) Top view (b) Bottom view.

4. RESULTS AND DISCUSSIONS

The U.S. Federal Communications Commission (FCC) allotted the frequency band 3.1–10.6 GHz for unlicensed commercial UWB communications. The proposed antenna covered the entire UWB range of 3.1–10.6 GHz and was extended up to 17.669 GHz. The elliptical UWB antenna used as reference was having lengths of semi-major axis and semi-minor axis as 9.0 mm and 7.0 mm respectively. By keeping a_1 fixed at 9.0 mm, the a_2 was varied as 8.5 mm, 8.0 mm and 7.5 mm. Even at $a_2 = 7.5$ mm, the antenna exhibited similar radiation properties as that of the original elliptical antenna. The patch area of reference elliptical antenna was 197.82 mm^2 and for the DEMPA with $a_2 = 7.5$ mm, it is found to be 181.335 181.335 mm^2 and thus achieved a miniaturization of 8.33%. Simulation results for DEMPA with the value of a_2 as 8.5 mm, 8.0 mm and 7.5 mm are given below. Experimental and simulation results for DEMPA with $a_2 = 7.5$ mm are compared. Performance comparison of the original elliptical antenna with the DEMPA with a_2 =7.5 mm was also carried out.

4.1. Antenna Return Loss

The variation of S_{11} parameter with change in a_2 as obtained from simulations is shown in Fig. 4. It is observed that the return loss characteristics were similar when the a_2 was reduced from 9.0 mm to 7.5 mm. The a_2 =9.0 mm corresponds to the original EMPA and $a_2 = 7.5$ mm corresponds to DEMPA. The Fig. 5 shows the comparison of Return Loss characteristics of simulated and fabricated DEMPA. Hence, it is evident that this technique can be used for antenna miniaturization. The closeness of simulated and manufactured antenna is also demonstrated by the Fractional Bandwidth (FB). The FB of antenna is its bandwidth divided by the centre frequency and it is a good measure of assessing how wideband the antenna is.

$$\text{FB} = \left(\frac{\text{Upper Frequency} - \text{Lower Frequency}}{\text{Centre Frequency}}\right) \times 100\% \tag{3}$$

where,

$$\text{the Centre Frequency} = \left(\frac{\text{Upper Frequency} + \text{Lower Frequency}}{2}\right) \tag{4}$$

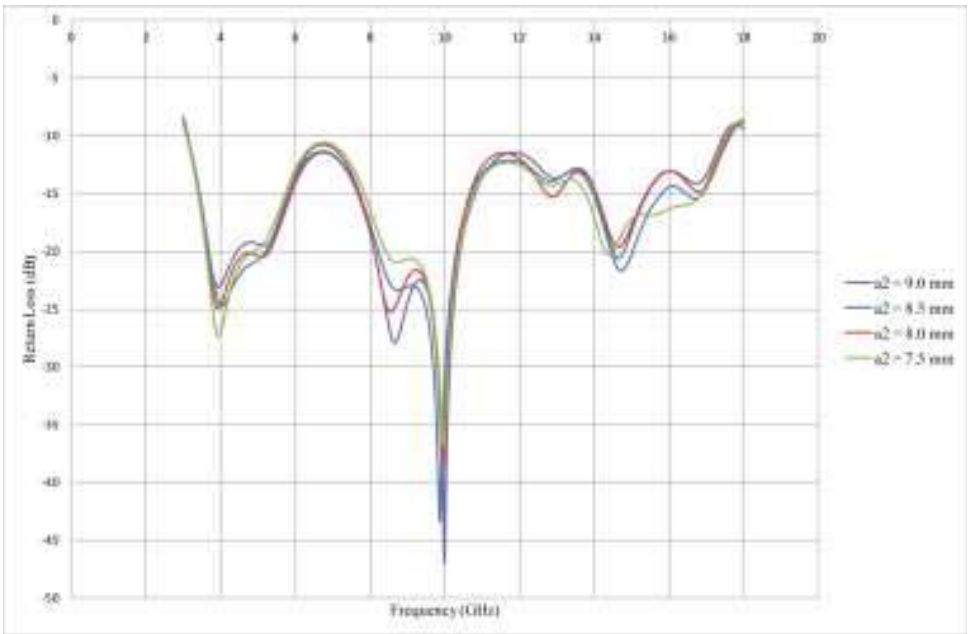

Figure 4. Comparison of simulated S_{11} parameter values for DEMPA with $a_2 = 8.5$ mm, 8.0 mm and 7.5 mm.

The upper and lower frequencies for DEMPA with $a_2 = 7.5\,\text{mm}$ as obtained from simulation are 17.175 GHz and 3.525 GHz, respectively. Hence, its centre frequency is 10.5 GHz and FB is 131.88%. For the manufactured DEMPA with $a_2 = 7.5\,\text{mm}$, the upper and lower frequencies are 17.669 GHz and 3.07 GHz respectively. Hence, its centre frequency is 10.37 GHz and FB becomes 134.07%. In other words, the simulation results show that DEMPA with $a_2 = 7.5\,\text{mm}$ covers the bandwidth of 131.88% from 3.07 GHz to 17.669 GHz for $|S_{11}| < -10\,\text{dB}$ Similarly, the manufactured DEMPA with $a_2 = 7.5\,\text{mm}$ covers the bandwidth of 134.07% from 3.525 GHz to 17.175 GHz for $|S_{11}| < -10\,\text{dB}$. The percentage error between simulated and measured FBs is found to be 1.63% .

Fig. 5 also shows the resonant frequencies identified for the antenna. There are six such resonant frequencies identified, and they are denoted as f_1, f_2, f_3, f_4, f_5 and f_6 for the fabricated antenna. The values of f_1, f_2, f_3, f_4, f_5, and f_6 are 4.43 GHz, 7.28 GHz, 9.00 GHz, 12.30 GHz, 14.33 GHz, and 16.43 GHz, respectively, and the corresponding frequency values for the simulated antenna are 3.96 GHz, 8.51 GHz, 10.01 GHz, 12.79 GHz, 14.64 GHz, and 16.70 GHz, respectively. The differences between simulated and measured resonant frequencies at the respective points are calculated to be −0.47 GHz, 1.23 GHz, 1.01 GHz, 0.49 GHz, 0.31 GHz, and 0.27 GHz. It is observed that the resonant frequencies of fabricated antenna are shifted towards right with respect to its corresponding values from simulation, except for 'f_1'. This difference between simulated and measured results may be due to the tolerance levels adopted during fabrication of antenna and welding of SMA connector, the ground plane effect and/or SMA connector effect. These aspects were not considered during simulations. Also, during the simulation, the dielectric loss tangent of FR-4 substrate was kept constant though it is a function of frequency.

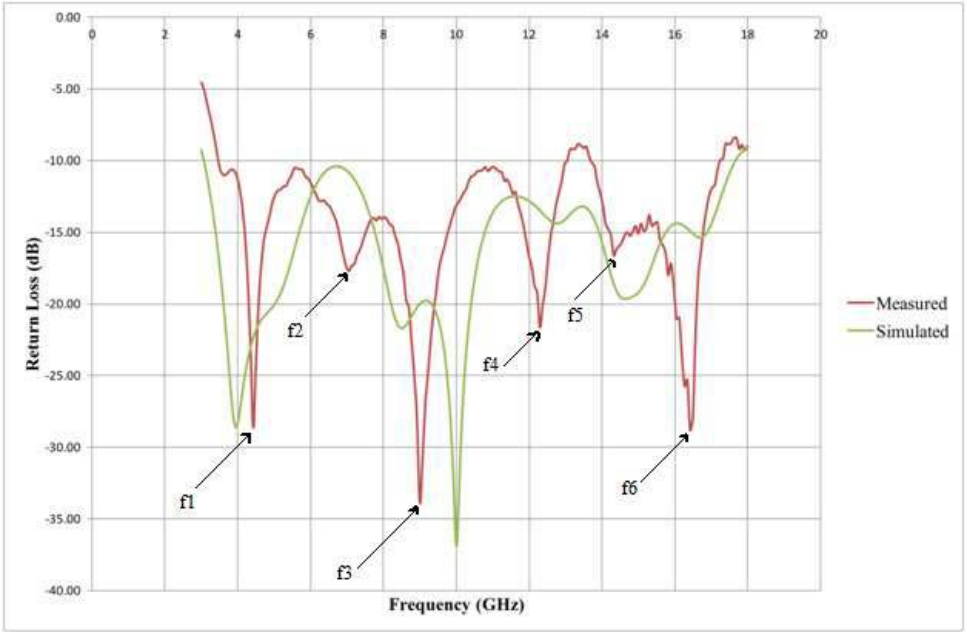

Figure 5. Comparison of return loss characteristics of simulated and manufactured DEMPA.

4.2. Radiation Patterns

Simulated far-field radiation patterns (at E-plane) of DEMPA with $a_2 = 7.5\,\text{mm}$ at resonant frequencies of 3.96 GHz, 8.51 GHz, 10.01 GHz, 12.79 GHz, 14.64 GHz, and 16.70 GHz with the azimuthal angle $\emptyset = 90^\circ$ are shown in Fig. 6. It is clear from these patterns that the antenna is directional. At 3.96 GHz, the pattern resembles to 8-shape. It is found that the radiation pattern is near to omnidirectional at 10.01 GHz where the return loss is the minimum. The Fig. 7 shows the 3-D polar plot of DEMPA with $a_2 = 7.5\,\text{mm}$ which represents the E-field at 3.96 GHz.

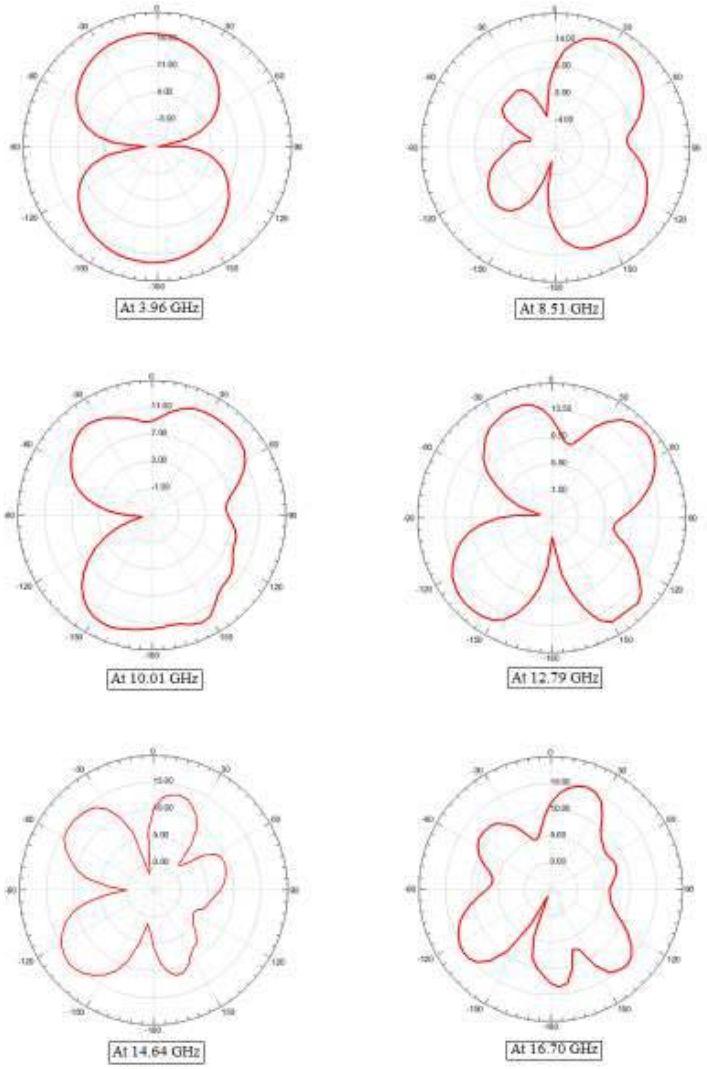

Figure 6. Simulated Radiation Patterns (at E-plane) for DEMPA with $a_2 = 7.5\,\text{mm}$ at resonant frequencies of 3.96 GHz, 8.51 GHz, 10.01 GHz, 12.79 GHz, 14.64 GHz and 16.70 GHz. The azimuthal angle, $\emptyset = 90°$.

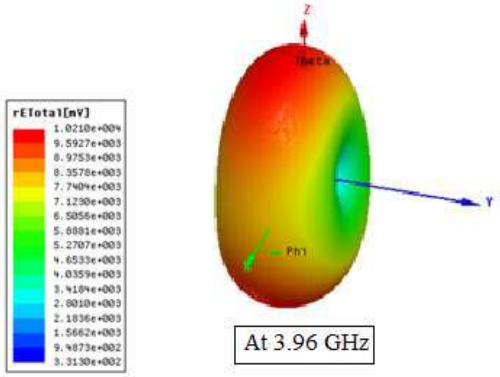

Figure 7. The 3-D polar plot for DEMPA with $a_2 = 7.5\,\text{mm}$ at resonant frequency of 3.96 GHz.

4.3. Surface Current Distributions

Fig. 8 shows the simulated surface currents over the patch and ground plane for the DEMPA with $a_2 = 7.5\,\text{mm}$ at the resonant frequencies of 3.96 GHz, 8.51 GHz, 10.01 GHz, 12.79 GHz, 14.64 GHz, and 16.70 GHz. These images are taken as looking on the patch and ground plane from the negative z axis as the maximum current will be underside of patch and ground plane. A common scale is provided on left side in each row for the ease of comparison. It is evident from Fig. 8 that the quantity of current is different at different resonant frequencies. At all the frequencies, the maximum current is found to be at the lower portion of patch and on the feed line. But, at 16.70 GHz, more than 50% of the boundary of patch bears maximum currents. It is understood that the effect of geometry of patch is more significant at 16.70 GHz. The 14.64 GHz comes next to this and here around 50% of the patch boundary bears the maximum current. It may be concluded that, in general, the distribution of surface current over the patch is increasing with increase in frequency and at the lower resonant frequencies, the current is more concentrated at the bottom portion of patch.

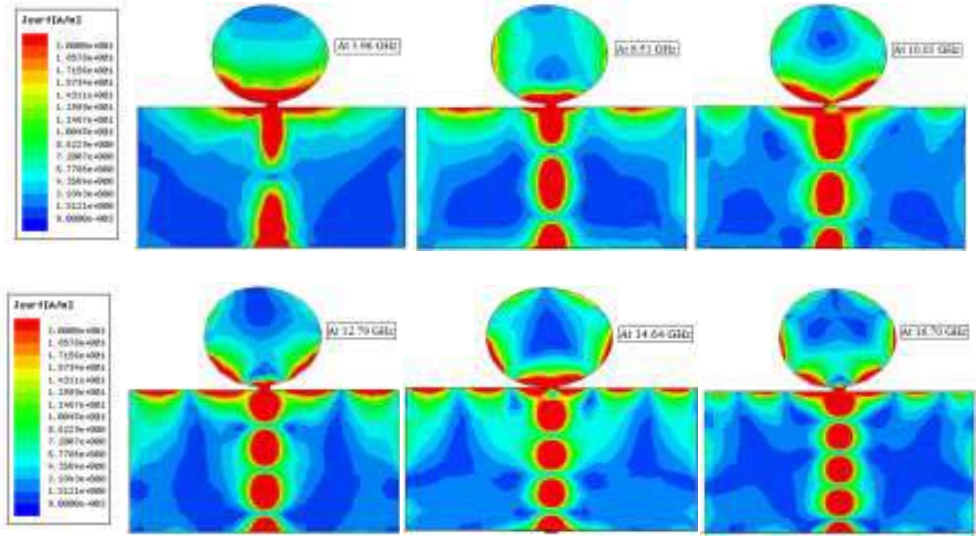

Figure 8. Simulated surface current distributions of DEMPA with $a_2 = 7.5\,\text{mm}$ at resonant frequencies of 3.96 GHz, 8.51 GHz, 10.01 GHz, 12.79 GHz, 14.64 GHz and 16.70 GHz as looking from the negative z axis.

4.4. VSWR Curves

The VSWR values for DEMPA with $a_2 = 8.5\,\text{mm}$, 8.0 mm, and 7.5 mm from simulations were < 2, and Fig. 9 shows their comparison.

For DEMPA with $a_2 = 7.5\,\text{mm}$, the measured and simulated values of VSWR were very close, and Fig. 10 shows their closeness. In the case of fabricated antenna, it is clear from Fig. 10 that VSWR values at the resonant frequencies such as 4.43 GHz, 9.0 GHz, 12.30 GHz, and 16.43 GHz are near unity. The measured values of VSWR at these frequencies were 1.07, 1.04, 1.19, and 1.07, respectively. The fact that these values are very close to unity indicates a good impedance match between the antenna and feed network.

4.5. Axial Ratio

Polarization of antenna is one of the important design considerations. When the transmitting and receiving stations use antennas of identical polarization, the signal strength obtained will be the maximum. Axial ratio tells us about the polarization of antenna. It is the ratio of minor and major axes of the polarization ellipse. An antenna is said to be linearly polarized when its axial ratio is $> 3\,\text{dB}$, and circularly polarized when axial ratio is $\leq 3\,\text{dB}$. For DEMPAs with $a_2 = 8.5\,\text{mm}$, 8.0 mm and 7.5 mm, the

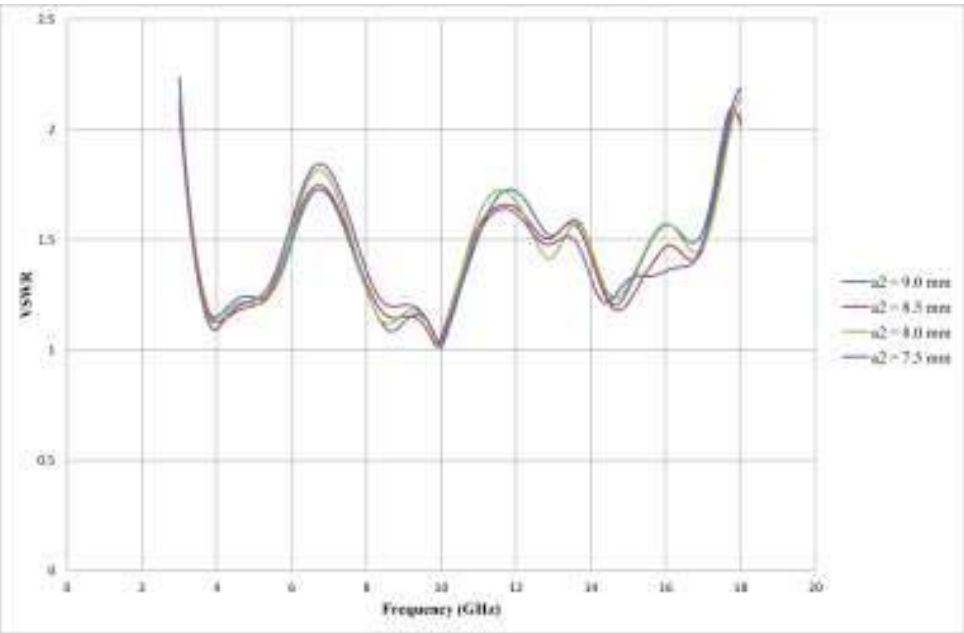

Figure 9. VSWR curves for DEMPA with $a_2 = 8.5\,\text{mm}$, 8.0 mm and 7.5 mm from simulations.

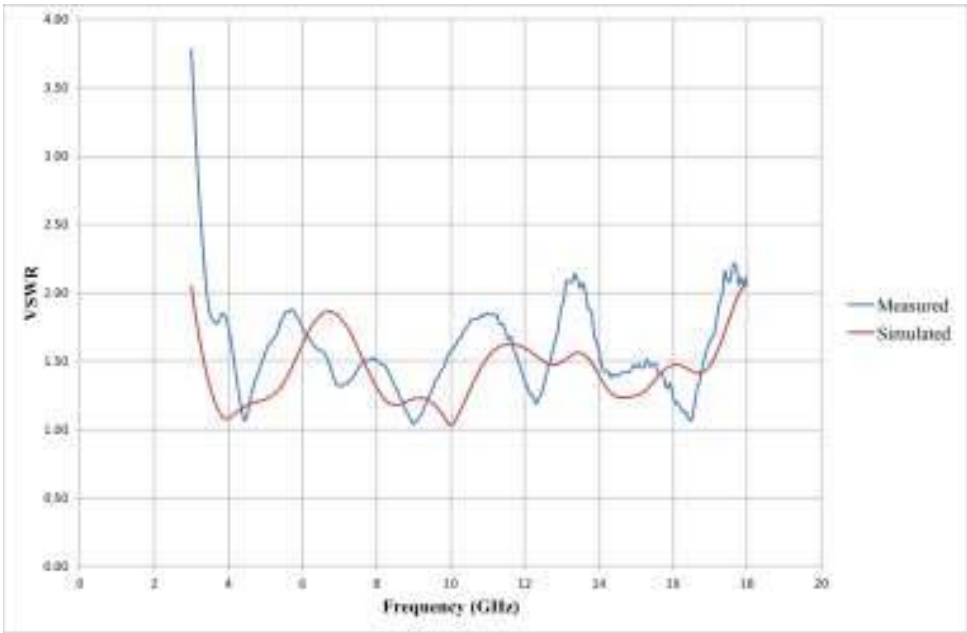

Figure 10. Measured and simulated VSWR for DEMPA with $a_2 = 7.5\,\text{mm}$.

axial ratio values were greater than 9 and hence these are turned out to be linearly polarized antennas. The Fig. 11 shows the axial ratio curve for DEMPA with $a_2 = 7.5\,\text{mm}$.

4.6. Gain Curves

Over the entire working band of 3.07 GHz–17.669 GHz, the peak gain is found to be positive and reasonable. Fig. 12 shows the curve for Peak gain in dB for DEMPA with $a_2 = 7.5\,\text{mm}$ obtained from simulations. The maximum and minimum values of peak gain were found to be 5.2 dB and 1.7 dB at

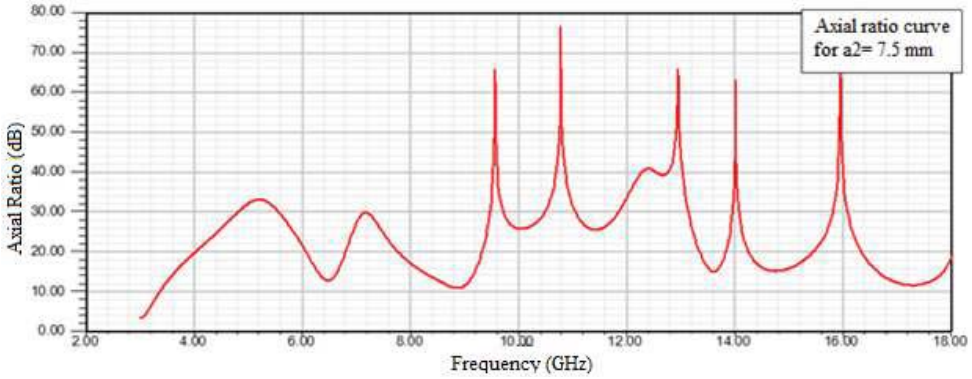

Figure 11. Axial ratio curve for DEMPA with $a_2 = 7.5$ mm.

15.1 GHz and 3.6 GHz respectively.

The proposed DEMPAs with $a_2 = 8.5$ mm, 8.0 mm, and 7.5 mm were found to have similar radiation properties as that of the reference EMPA [17] and cover the entire UWB even if their effective patch areas are less. For DEMPA with $a_2 = 7.5$ mm, the extent of miniaturization is the maximum with the percentage reduction in the effective patch area becoming 8.33%. The resulting antennas are linearly polarized.

In comparison with several other MSPAs working in the UWB range, the DEMPA is found to have less effective patch area, and this is a clear indication of attaining the goal of antenna miniaturization. For the proposed DEMPA, the patch area is 181.335 mm^2, and its comparison with other MSP antennas in UWB range is shown in Table 1 below.

Table 1. Comparison of effective patch area of the proposed DEMPA with that of various patch antennas from literature.

Reference	Antenna size details (mm)	Antenna design details	Effective patch area (mm^2)	Published year
[35]	$a = 10.0$; $b = 9.0$	Elliptical patch	282.6	2005
[36]	$a = 60.0$; $b = 15.0$	Half elliptical patch	942	2007
[15]	$a = 13.5$; $b = 9.0$; $r = 7.0$	Crescent shaped patch	227.65	2007
[17]	$a = 9.0$; $b = 7.0$; $t = 6.16$	Slot loaded elliptical patch	191.66	2009
[37]	$a = 15.0$; $b = 10.0$; $R = 8.0$	Circular slot in ellipse with stub	745.534	2009
[38]	$a = 10.92$; $b = 7.80$	U slot in elliptical patch	257.253	2010
[11]	$a = 19.6$; $b = 14.0$; $t = 0.6$	Elliptical patch with two slots	188.791	2010
[39]	$a = 60.0$; $b = 15.0$	Elliptical patch	1884	2011
[40]	$a = 3.0$; $b = 1.5$; $R = 9.0$	Elliptical slot in circular patch	240.21	2016
[41]	$W = 15.0$; $L = 14.5$; $R = 2.0$	Four Corner cuts in rectangular patch	204.94	2018
[42]	$W = 17.6$; $L = 14.1$; $L_1 = 6.4$	Trapezoidal patch with three slots	183.43	2018
[43]	$r_1 = 26.5$; $r_2 = 23.25$	Elliptical patch	1934.63	2018
[44]	$a = 17.0$; $b = 8.5$	U slot in elliptical patch	444.175	2019
Proposed by authors	$a_1 = 9.0$; $a_2 = 7.5$; $b = 7.0$	Double-elliptical patch	181.335	
Where, a = length of semi-major axis of ellipse; b = length of semi-minor axis of ellipse; R = radius; W = width; L = length; t = slot width. All dimensions are in mm.				

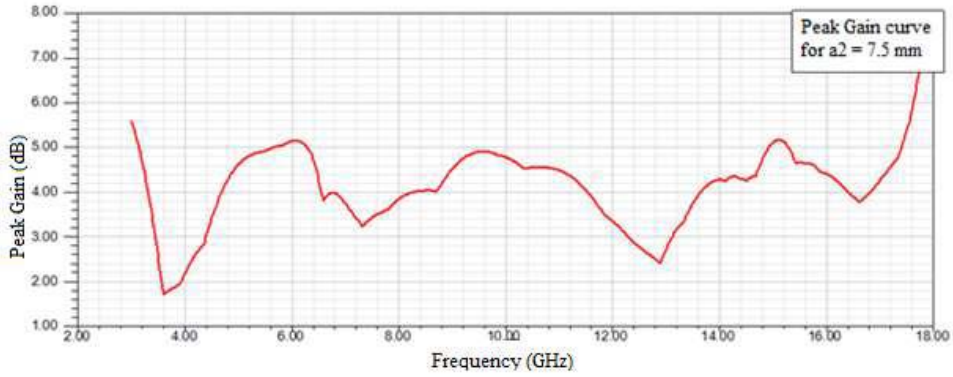

Figure 12. Peak gain curve for DEMPA with $a_2 = 7.5\,\text{mm}$ from simulation.

5. CONCLUSION

In view of the increasing requirements from commercial Micro-Strip Patch Antenna industry for greater design flexibility and miniaturization of effective patch area, a novel shaped patch antenna, called Double-Elliptical Micro-strip Patch Antenna (DEMPA) is proposed for UWB applications. The innovations in the proposed method are the emergence of an additional degree of freedom for the design of elliptical shaped patch antenna and reduction in effective patch area even without losing its radiation properties. In the present work, the length of semi-major axis for the right hand side half-elliptical patch (a_2) of DEMPA was varied to attain miniaturization. The DEMPA with $a_2 = 7.5\,\text{mm}$ was fabricated and tested. There was good agreement between the simulated and measured performance parameters of antenna. The important findings are given below.

(i) The DEMPA can be used for greater design flexibility as there is an additional degree of freedom compared to elliptical patch antenna.

(ii) For DEMPA with $a_2 = 7.5\,\text{mm}$, the reduction in effective patch area was 8.33% in comparison with reference EMPA. This was achieved even while retaining the similar radiation properties. Hence, the DEMPA can be used for antenna miniaturization.

(iii) All the three DEMPAs were found to be covering the entire frequency range for UWB. For DEMPA with $a_2 = 7.5\,\text{mm}$, the band is found to be extended up to 17.669 GHz. Hence, this antenna is suitable for radiolocation applications, mobile applications, fixed satellite communications, and space research.

REFERENCES

1. Shen, L., "The elliptical microstrip antenna with circular polarization," *IEEE Trans. Antennas Propag.*, Vol. 29, No. 1, 90–94, Jan. 1981.
2. Kumprasert, N., "Theoretical study of dual-resonant frequency and circular polarization of elliptical microstrip antennas," *IEEE Antennas and Propagation Society International Symposium. Transmitting Waves of Progress to the Next Millennium. 2000 Digest. Held in conjunction with: USNC/URSI National Radio Science Meeting (C*, Vol. 2, 1015–1020, 2000.
3. Raheja, D., B. Kanaujia, and S. Kumar, "A dual polarized triple band stacked elliptical microstrip patch antenna for WLAN applications," *Wirel. Pers. Commun.*, Vol. 100, Apr. 2018.
4. Peddakrishna, S. and T. Khan, "Performance improvement of slotted elliptical patch antenna using FSS superstrate," *Int. J. RF Microw. Comput.-Aided Eng.*, Vol. 28, No. 9, e21421, 2018.
5. Kashyap, N., "Circular slotted elliptical patch antenna with elliptical notch in ground," *Progress In Electromagnetics Research C*, Vol. 74, 181–189, 2017.

6. Eshtiaghi, R., J. Nourinia, and C. Ghobadi, "Electromagnetically coupled band-notched elliptical monopole antenna for UWB applications," *IEEE Trans. Antennas Propag.*, Vol. 58, No. 4, 1397–1402, Apr. 2010.
7. Dastranj, A., "Very small planar broadband monopole antenna with hybrid trapezoidal-elliptical radiator," *Antennas Propag. IET Microw.*, Vol. 11, No. 4, 542–547, 2017.
8. Gupta, M. and V. Mathur, "Multiband multiple elliptical microstrip patch antenna with circular polarization," *Wirel. Pers. Commun.*, Vol. 102, No. 1, 355–368, Sep. 2018.
9. Garhwal, A., et al., "Circular and elliptical shaped fractal patch antennas for multiple applications," *Int. J. Eng. Adv. Technol. IJEAT*, Vol. 8, No. 5, 114–120, Jun. 2019.
10. Sharma, V., V. K. Saxena, K. B. Sharma, and D. Bhatnagar, "Radiation performance of an elliptical patch antenna with three orthogonal sector slots," *Romanian J. Inf. Sci. Technol.*, Vol. 14, No. 2, 123–130, Nov. 2011.
11. Zhou, R., Z. Wu, H. Xin, and R. W. Ziolkowski, "Designs of ultra wideband (UWB) printed elliptical monopole antennas with slots," *Microw. Opt. Technol. Lett.*, Vol. 52, 466–471, Feb. 2010.
12. Ahmed, E. S. and M. Q. Mohammed, "A novel compact size dual notched bands uwb elliptical monopole antenna," *Int. J. Eng. Adv. Technol. IJEAT*, Vol. 2, No. 6, 176–181, Aug. 2013.
13. Tilak, G. B. G., S. K. Kotamraju, B. T. P. Madhav, C. Sri Kavya, and M. V. Rao, "Broken heart shaped monopole antenna for WiMAX applications," *Int. J. Recent Technol. Eng. IJRTE*, Vol. 8, No. 2, 2333–2337, Jul. 2019.
14. Krishna, T. V. R., et al., "Design and study of a CPW fed truncated circular patch switchable band-notched UWB antenna," *Int. J. Recent Technol. Eng. IJRTE*, Vol. 8, No. 1, 3037–3043, May 2019.
15. Azenui, N. C. and H. Y. D. Yang, "A printed crescent patch antenna for ultrawideband applications," *IEEE Antennas Wirel. Propag. Lett.*, Vol. 6, 113–116, 2007.
16. Younssi, M., A. Jaoujal, A. E. Moussaoui, and N. Aknin, "Miniaturized probe-fed elliptical microstrip patch antenna for radiolocation applications," *Int. J. Eng. Technol.*, Vol. 14, No. 5, 324–327, Nov. 2012.
17. Peng, L., C. Ruan, and X. Yin, "Analysis of the small slot-loaded elliptical patch antenna with a band-notched for UWB applications," *Microw. Opt. Technol. Lett.*, Vol. 51, No. 4, 973–976, 2009.
18. Shrama, B., V. Sharma, K. B. Sharma, and D. Bhatnagar, "Broadband semielliptical patch antenna with semicircular ring slot for WiMax application," *Chinese Journal of Engineering*, 2014, [Online] Available: https://www.hindawi.com/journals/cje/2014/379073/, Accessed: 13-Sep-2019.
19. Bhattacharyya, A. K. and L. Shafai, "Theoretical and experimental investigation of the elliptical annular ring antenna," *IEEE Trans. Antennas Propag.*, Vol. 36, No. 11, 1526–1530, Nov. 1988.
20. Rokunuzzaman, M., R. Azim, N. Misran, M. F. Asillam, and M. Islam, "Development of a semielliptical partial ground plane antenna for RFID and GSM-900," *Int. J. Antennas Propag.*, Vol. 2014, 7, Apr. 2014.
21. Griffiths, L. A., C. Furse, and Y. C. Chung, "Broadband and multiband antenna design using the genetic algorithm to create amorphous shapes using ellipses," *IEEE Trans. Antennas Propag.*, Vol. 54, No. 10, 2776–2782, Oct. 2006.
22. Sekra, P., S. Shekhawat, M. Dubey, D. Bhatnagar, V. K. Saxena, and J. S. Saini, "Design of circularly polarized edge truncated elliptical patch antenna with improved performance," *IJRSP*, Vol. 404, Aug. 2011.
23. Dey, S., "Symmetrical Slot Loaded Dual Band Elliptical Microstrip Patch Antenna'.
24. Mishra, S. N., D. Konhar, D. Mishra, and R. K. Mishra, "On the possibility of linear polarization in elliptical microstrip patch antenna," *Microw. Opt. Technol. Lett.*, Vol. 61, No. 4, 1048–1051, Apr. 2019.
25. Donelli, M. and F. Robol, "Circularly polarized monopole hook antenna for ISM-band systems," *Microw. Opt. Technol. Lett.*, Vol. 60, No. 6, 1452–1454, 2018.

26. Donelli, M., T. Moriyama, and M. Manekiya, "A compact switched-beam planar antenna array for wireless sensors operating at Wi-Fi band," *Progress In Electromagnetics Research C*, Vol. 83, 137–145, 2018.
27. Donelli, M. and P. Febvre, "An inexpensive reconfigurable planar array for Wi-Fi applications," *ProgresS IN Electromagnetics Research C*, Vol. 28, 71–81, 2012.
28. Donelli, M., I. J. Craddock, D. Gibbins, and M. Sarafianou, "A three-dimensional time domain microwave imaging method for breast cancer detection based on an evolutionary algorithm," *Progress In Electromagnetics Research M*, Vol. 18, 179–195, 2011.
29. Alkurt, F. O. and M. Karaaslan, "Pattern reconfigurable metasurface to improve characteristics of low profile antenna parameters," *Int. J. RF Microw. Comput.-Aided Eng.*, e21790, 2019.
30. Alkurt, F. O., et al., "Enhancement of image quality by using metamaterial inspired energy harvester," *Phys. Lett. A*, 126041, Oct. 2019.
31. Esen, M., I. Ilhan, M. Karaaslan, and R. Esen, "Investigation of electromagnetic and ultraviolet properties of nano-metal-coated textile surfaces," *Appl. Nanosci.*, 1–11, Aug. 2019.
32. Alkurt, F. O. and M. Karaaslan, "Characterization of tunable electromagnetic band gap material with disordered cavity resonator for X band imaging applications by resistive devices," *Opt. Quantum Electron.*, Vol. 51, No. 8, 279, Aug. 2019.
33. Derın, O., M. Karaaslan, E. Ünal, F. Karadağ, O. Altintaş, and O. Akgöl, "Exhibition of polarization conversions with asymmetric transmission theory, natural like chiral, artificial chiral nihility and retrieval studies for K- and C-band radar applications," *Bull. Mater. Sci.*, Vol. 42, No. 4, 191, Jun. 2019.
34. Ozturk, M., O. Akgol, U. K. Sevim, M. Karaaslan, M. Demirci, and E. Unal, "Experimental work on mechanical, electromagnetic and microwave shielding effectiveness properties of mortar containing electric arc furnace slag," *Constr. Build. Mater.*, Vol. 165, 58–63, Mar. 2018.
35. Huang, C.-Y. and W.-C. Hsia, "Planar elliptical antenna for ultra-wideband communications," *Electron. Lett.*, Vol. 41, No. 6, 296–297, Mar. 2005.
36. Yan, X.-R., S.-S. Zhong, and X.-L. Liang, "Compact printed semi-elliptical monopole antenna for super-wideband applications," *Microw. Opt. Technol. Lett.*, Vol. 49, No. 9, 2061–2063, 2007.
37. Jiao, S., N. Ge, J. Lu, and M. Jiang, "Monopole crescent elliptical antenna with band-notched characteristics for UWB applications," *Tsinghua Sci. Technol.*, Vol. 14, No. 4, 460–464, Aug. 2009.
38. Panda, J. R. and R. S. Kshetrimayum, "A planar microstrip-line fed elliptical UWB 5.2 GHz/5.8 GHz notch antenna with U-shaped slot," *2010 International Conference on Computer and Communication Technology (ICCCT)*, 806–811, 2010.
39. Liu, J., S. Zhong, and K. P. Esselle, "A printed elliptical monopole antenna with modified feeding structure for bandwidth enhancement," *IEEE Trans. ANTENNAS Propag.*, Vol. 59, No. 2, 667–670, Feb. 2011.
40. Meena, M. L., M. Kumar, G. Parmar, and R. S. Meena, "Design analysis and modeling of directional UWB antenna with elliptical slotted ground structure for applications in C- & X-bands," *Progress In Electromagnetics Research C*, Vol. 63, 193–207, 2016.
41. Awad, N. M. and M. K. Abdelazeez, "Multislot microstrip antenna for ultra-wide band applications," *J. King Saud Univ. — Eng. Sci.*, Vol. 30, No. 1, 38–45, Jan. 2018.
42. Debab, M. and Z. Mahdjoub, "Characteristics UWB Planar Antenna with dual notched bands for WIMAX and WLAN," *Adv. Electromagn.*, Vol. 7, No. 5, 20–25, Sep. 2018.
43. Mansoul, A. and F. Ghanem, "Frequency reconfigurable antenna for cognitive radios with sequential UWB mode of perception and multiband mode of operation," *Int. J. Microw. Wirel. Technol.*, Vol. 10, No. 9, 1096–1102, Nov. 2018.
44. Rao, D S., I Govardhani, T. Harish, P. V. Rao, K. Raviteja, and L. K. Rao, "A simple reconfigurable elliptical UWB antenna with dual band rejection," *Int. J. Innov. Technol. Explor. Eng.*, Vol. 8, No. 7, 813–815, May 2019.